

# Material optimization via optical and spectroscopic parameters of $\text{Al}_2\text{O}_3:\text{Er}^{3+}$ for the development of amplifiers and lasers

D. B. Bonneville, C. E. Osornio-Martinez, M. Dijkstra and S. M. García-Blanco

Integrated Optical Systems, MESA+ Institute for Nanotechnology, University of Twente, 7500 AE Enschede, The Netherlands.

*In this work, we report on the optical and spectroscopic optimization of  $\text{Al}_2\text{O}_3:\text{Er}^{3+}$  for the development of amplifiers and lasers by providing details on optical processes in the material such as luminescent lifetimes, signal enhancement, and propagation and absorption losses. In this manner we intend to optimize the host material for favourable  $\text{Er}^{3+}$  transitions to maximize the available net gain at 1550 nm, when pumped at 1480 nm. By measuring and tracking a variety of parameters across fabrication and treatment steps, ideal methods are discovered for maximizing optical gain in  $\text{Al}_2\text{O}_3:\text{Er}^{3+}$  waveguides.*

## Introduction

Photonic integrated circuits (PICs) are becoming widespread in their research and application to alleviate a variety of limitations in fields such as sensing, telecommunications, quantum information and LIDAR (light-detection and ranging). Monolithic (integrated on one chip) photonic devices however still require high power, stable-linewidth emission sources to enable key components in a variety of applications. To address this, new materials are required to provide optical gain that can be integrated on to the silicon platform. Although III-V materials provide direct bandgap transitions and electrical pumping, they suffer from drawbacks such as power and noise limitations, as well as complicated and costly processing like epitaxy and wafer-bonding. Rare-earth ions can be integrated into materials several ways including ion implantation [1], gas precursors via atomic layer deposition (ALD) [2], and solid targets during sputtering [3]. Reactive magnetron sputtering is a readily scalable technique which provides wafer processing and relatively fast deposition rates on a variety of substrates.  $\text{Al}_2\text{O}_3$  has been demonstrated to be a suitable host for rare-earth ions, including  $\text{Er}^{3+}$  and  $\text{Yb}^{3+}$  [3–5] leading to on-chip amplifier and lasers. In this work we demonstrate  $\text{Al}_2\text{O}_3:\text{Er}^{3+}$  waveguide amplifiers fabricated via reactive magnetron sputtering and electron-beam lithography (EBL). Annealing is demonstrated to decrease the background propagation losses of fabricated samples. The refractive index and photoluminescent lifetimes (PL) for a variety of films are shown, before and after annealing at multiple temperatures for two different concentrations. Pumping at 1480 nm was used to produce on-chip gain, which is shown for the small signal regime, and for high signal powers at 1532 and 1550 nm. It is revealed through lifetime, signal enhancement (SE) and loss measurements that annealing enables gain for fabricated samples up to a limit, which is  $\text{Er}^{3+}$  concentration dependent. Pathways and prospects for improvement are discussed.

## Fabrication

Films were deposited in the MESA+ clean-room facilities using reactive magnetron sputtering following procedures outlined in [6]. Films reported in this work vary in  $\text{O}_2$  flow from approximately 2.8–3.2 sccm with deposition rates of  $\sim 4$  nm/min and stage temperatures up to  $760^\circ\text{C}$ . Erbium concentrations are approximately known using calibrated sputtering powers based on Rutherford backscattering measurements (RBS). Samples were stored in  $\text{N}_2$  ambient in between fabrication steps to avoid OH<sup>-</sup> contamination. Electron-beam lithography (EBL) was used to pattern negative resist at a dose of  $1000 \mu\text{C}/\text{cm}^2$  to be used as an etch mask for the definition of spirals, ring

resonators and straight waveguides for signal enhancement and loss characterization. Nanotapers with widths and lengths of 0.15 and 2000  $\mu\text{m}$  were designed and optimized for 1480 nm coupling which were included to increase on-chip pump power. Reactive ion-etching (RIE) was performed to define the waveguides with 25 and 10 sccm of  $\text{BCl}_3$  and  $\text{HBr}$  gas flows respectively at a chamber pressure of 3 mTorr and 25 W RF power. Plasma-enhanced chemical vapour deposition (PECVD) was used to deposit a  $\text{SiO}_2$  cladding at a deposition rate of 37 nm/min using 200 and 710 sccm of  $\text{SiH}_4/\text{N}_2$  and  $\text{N}_2\text{O}$  respectively, with a chamber pressure of 650 mTorr at 300  $^\circ\text{C}$  stage temperature and 60 W of power. Chips were diced and measured before and after annealing in a tube furnace in  $\text{N}_2$  ambient. Film thicknesses of  $\sim 800$  nm and waveguide widths of 1.6  $\mu\text{m}$  were used for the majority of the work demonstrated.

## Characterization

Waveguides and films were characterized as fabricated and after annealing in order to track the optimal parameters for gain as they develop for a variety of temperatures. Films were measured with prism coupling before patterning revealing losses from  $\sim 0.9$ –1.6 dB/cm at 636 nm for the samples presented here. Ring resonator samples were measured at  $>1600$  nm in order to track the background propagation losses in between annealing steps, as shown in Fig. 1 a) for the starred sample with an  $\text{Er}^{3+}$  ion concentration of  $2.9 \times 10^{20}/\text{cm}^3$ , which was annealed at 500  $^\circ\text{C}$ . Figure 1b) demonstrates increasing refractive index and lifetime measured in films with variable angle spectroscopic ellipsometry (VASE) and 976 nm pumping respectively as deposition set stage temperature rises. Shown in the inset is a sample PL measurement as well as lifetime for two different concentrations across annealing temperatures. Figure 1c) shows the lifetime setup, which was measured using a 976 nm pump diode and a 10 Hz modulation source with back reflected ASE signal. Powers were kept low to ensure that reabsorption and reemission of the signal or unwanted excitation was not occurring following methods described in [7]. Methods from [1] were used to assess and fit the data.

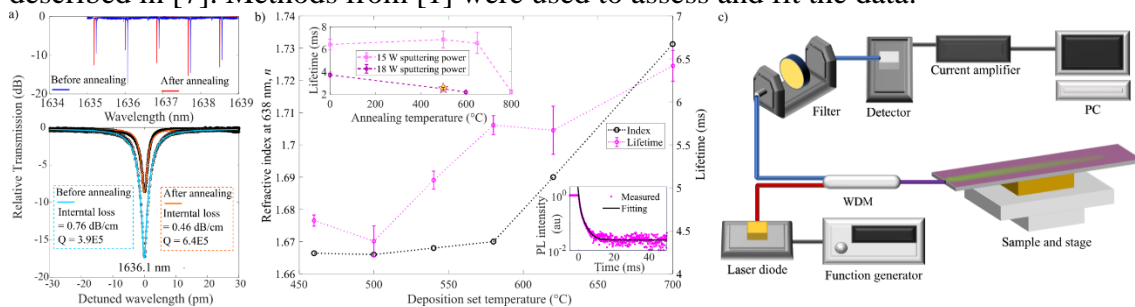


Figure 1. a) Ring resonator measurements for a 1.3  $\mu\text{m}$  wide, 786 nm thick waveguide with a gap of 1.3  $\mu\text{m}$  and radii of 300  $\mu\text{m}$ , with 18 W sputtering power before and after annealing at 500  $^\circ\text{C}$ . b) Refractive index and lifetime for a variety of deposition temperatures with inset sample PL measurement (bottom right) and lifetime vs annealing temperature for films with 15 and 18 W sputtering power (top left). c) PL lifetime measurement setup including a 976 nm laser diode,  $<1100$  nm blocking filter and 980/1550 WDM.

A decrease of 0.3 dB/cm is observed after annealing at 550  $^\circ\text{C}$  shown in Fig. 1a). As demonstrated in Fig. 1b), the deposition temperature has an impact on the lifetime and index of the alumina. Films shown in the inset were deposited at 760  $^\circ\text{C}$  to get the  $\text{Er}^{3+}$  lifetime closer to its intrinsic value  $\sim 7$ –8 ms. As shown in the inset, (top left) samples with higher  $\text{Er}^{3+}$  concentrations ( $1.6$  vs.  $2.9 \times 10^{20}/\text{cm}^3$ ) have lower lifetimes, likely due to clustering in the host and fast quenching of the luminescent decay. It is anticipated annealing the samples provides additional energy for the ions to redistribute in the host, allowing clusters to form, which would happen at lower thermal thresholds for higher

concentrations. The decrease of propagation losses due to the alumina host enables low-loss waveguides and potential for high gain amplifiers. Tracking the lifetime across annealing temperatures, as well as the propagation losses reveals ideal parameters to optimize the gain.

In order to quantify the on-chip gain for the devices, waveguide losses were measured as well as signal enhancement (SE). The starred sample from the inset (top left) in Fig. 1b) was used to characterize the gain. Figure 2a) demonstrates the setup used to pump and measure the samples for SE at high and low powers for 1532 and 1550 nm. Butterfly mounted 1480 nm diodes were used to pump the waveguides, and an erbium-doped fiber amplifier (EDFA) as well as a 1550 nm laser diode were used to measure high signal power gain for 1532 and 1550 nm respectively. For small signal gain the tunable laser was used without the EDFA in the setup. An optical spectrum analyzer (OSA) was used to detect signals and distinguish and correct for the amplified spontaneous emission (ASE) after passing through a low-pass filter. Polarization maintaining fibers were used with motor-controlled stages for alignment. Waveguide losses were measured using cut-back and an IR camera at 1532 and 1550 nm to avoid the ground-state excitation that can occur due to signal power build up during ring resonator measurements.

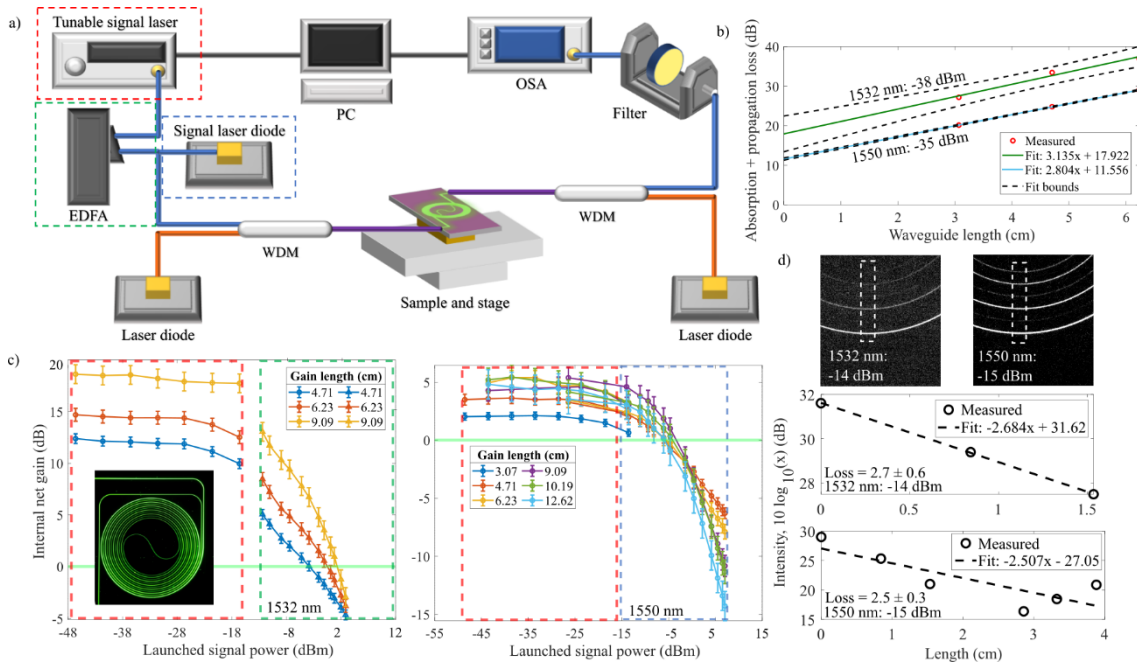


Figure 2. a) Pumping setup for measuring gain with three different source options including a tunable laser source, an EDFA and a high-power signal diode for small signal, and high power 1532 and 1550 nm measurements respectively. b) Cut-back loss measurements in varying spiral lengths. c) Internal net gain measurements for waveguide of varying length with 502 mW launched 1480 nm pump power for 1532 and 1550 nm varying signal powers. Inset included of sample during test. d) IR images of waveguide with 1532 and 1550 nm guided modes and obtained fits for loss verification.

Figure 2b) demonstrates the fits obtained from varying spiral lengths used for cutback loss estimations revealing total losses (absorption plus propagation) of  $\sim 3.1$  and  $2.8$  dB/cm for 1532 and 1550 nm respectively. On-chip peak (internal) gain of  $18.7$  dB for a  $9.09$  cm waveguide as well as  $2.6$  dB/cm for a  $4.71$  cm waveguide is shown in Fig. 2c) at 1532 nm. This is achieved with bi-directional pumping at  $1480$  nm ( $\sim 500$  mW launched pump power) to ensure large amounts of on-chip pump power and high signal power gain thresholds in comparison to enhanced energy-transfer up conversion (ETU)

with 980 nm pumping. To verify the losses used for gain calculations, IR camera images were used to measure the scattering while coupled in a spiral and used to extract the intensity as a function of length, shown in Fig 2d). The upper-bounded error result was used in both cases to calculate the gain, resulting in total loss subtractions of 3.2 and  $2.8 \pm 0.1$  dB/cm at 1532 and 1550 nm respectively from the SE measurements.

Future work aims at realizing new samples with varying concentrations and annealing steps to optimize the gain, similar to the study shown here. In parallel designs will be altered to measure devices without nano-tapers to study the influence of coupling loss at 1532 nm, which was considerably higher here than 1550 nm as seen in Fig. 2b). It is anticipated lower concentration samples will provide higher possible annealing temperatures before clustering and therefore lower achievable losses. After optimizing the gain material, the process will be applied to multi-layer waveguide systems for the realization of integrated amplifiers on laser cavity architectures.

## Conclusion

Waveguide losses, lifetime and on-chip gain was demonstrated on reactively sputtered  $\text{Al}_2\text{O}_3:\text{Er}^{3+}$  waveguides fabricated with EBL and RIE. Lifetime was shown to be deposition stage temperature dependent, while decreasing with annealing after a certain temperature depending on the concentration. Annealing was demonstrated to reduce propagation losses by 0.3 dB/cm for a sample with an ion concentration of  $2.9 \times 10^{20}/\text{cm}^3$ , which was subsequently measured for gain with 1480 nm pumping. Losses were measured via cutback and IR imaging, resulting in total losses of 3.2 and  $2.8 \pm 0.1$  dB/cm, which were subtracted from the SE data obtained by pumping. On-chip gain of 18.7 dB was achieved in a 9.09 cm long waveguide, as well as 2.64 dB/cm in a 4.71 cm long waveguide at 1532 nm for 502 mW launched pump power. Annealing and measuring lower concentration samples is promising to further reduce the losses and optimize the amplifier performance.

## Funding

This project has received funding from the European Union's Horizon 2020 research and innovation program under grant agreement No 101017136. This result reflects only the author's view and the European Commission is not responsible for any use that may be made of the information it contains.

## References

- [1] Y. Liu, et al., "A photonic integrated circuit-based erbium-doped amplifier," *Science*, vol. 376, 2022.
- [2] J. Rönn, et al., "Ultra-high on-chip optical gain in erbium-based hybrid slot waveguides," *Nature Communications*, vol. 10, no. 1, 2019.
- [3] W. A. P. M. Hendriks et al., "Rare-earth ion doped  $\text{Al}_2\text{O}_3$  for active integrated photonics," *Advances in Physics X*, vol. 6, no. 1, 2021.
- [4] S. A. Vázquez-Córdova et al., "Erbium-doped spiral amplifiers with 20 dB of net gain on silicon," *Optics Express*, vol. 22, no. 21, 2014.
- [5] J. D. B. Bradley et al., "Monolithic erbium- and ytterbium-doped microring lasers on silicon chips," *Optics Express*, vol. 22, no. 10, 2014.
- [6] C. I. Emmerik et al., "Relative oxidation state of the target as guide line for depositing optical quality RF reactive magnetron sputtered  $\text{Al}_2\text{O}_3$  layers," *Optical Materials Express*, vol. 10, no. 6, (2020).
- [7] R. Wang et al., "Erbium-ytterbium co-doped aluminum oxide thin films: Co-sputtering deposition, photoluminescence, luminescent lifetime, energy transfer and quenching fraction," *Optical Materials*, vol. 111, (2021).